Water adsorption properties of Fe(pz)[Pt(CN)4] and the Capture of CO2 and CO

Daniel Alvarado-Alvarado, Juan González-Estefan, Gabriel J. Flores, J. Raziel Álvarez, Julia Aguilar-Pliego, Alejandro Islas-Jácome, Guillaume Chastanet, Eduardo González-Zamora, Hugo A. Lara-García, Brenda Alcántar-Vázquez, et al.

Water adsorption properties of $Fe(pz)[Pt(CN)_4]$ and the capture of CO_2 and CO

Daniel Alvarado-Alvarado,[‡a] Juan H. González-Estefan,[‡b,c] J. Gabriel Flores,[a,d] J. Raziel Álvarez,[a] Julia Aguilar-Pliego,[d] Alejandro Islas-Jácome,[*e] Guillaume Chastanet,[b,c] Eduardo González-Zamora,[e] Hugo A. Lara-García,[f] Brenda Alcántar-Vázquez,[g] Mathieu Gonidec[*b,c] and Ilich A. Ibarra[*a]

[a] Laboratorio de Fisicoquímica y Reactividad de Superficies, Instituto de Investigaciones en Materiales, Universidad Nacional Autónoma de México, Circuito Exterior S/N, Ciudad Universitaria, C.P. 04510, Coyoacán, Ciudad de México, México.
[b] CNRS, ICMCB, UMR 5026, F-33600 Pessac, France.
[c] Univ. Bordeaux, ICMCB, UMR 5026, F-33600 Pessac, France.
[d] Departamento de Química Aplicada, Universidad Autónoma Metropolitana-Azcapotzalco, San Pablo 180, Col. Reynosa-Tamaulipas, Azcapotzalco, C.P. 02200, Ciudad de México, México.
[e] Departamento de Química, Universidad Autónoma Metropolitana-Iztapalapa, San Rafael Atlixco 186, Col. Vicentina, C.P. 09340, Iztapalapa, Ciudad de México, México.
[f] Instituto de Física, Universidad Nacional Autónoma de México, Circuito de la Investigación científica s/n, CU, Del. Coyoacán, 04510 Ciudad de México, México.
[g] Instituto de Ingeniería, Coordinación de Ingeniería Ambiental, Universidad Nacional Autónoma de México, Circuito Escolar s/n, CU, Del. Coyoacán, CP04510, Ciudad de México, México.
[‡]These authors contributed equally to this work.

ABSTRACT: H_2O and cyclohexane adsorption properties, as well as CO_2 and CO capture capability of the microporous material $Fe(pz)[Pt(CN)_4]$ were examined. This 3D coordination polymer retained its crystallinity and structural stability after all adsorption-desorption experiments (demonstrated by PXRD and BET surface area). Thus, the total water uptake was equal to 14.6 wt% (8.12 mmol g^{-1}) at 90 % P/P_0, and in comparison to the adsorption of cyclohexane, $Fe(pz)[Pt(CN)_4]$ demonstrated a relatively high degree of hydrophilicity. The total cyclohexane uptake of 0.28 mmol g^{-1}, which compared to the total water uptake value of 8.12 mmol g^{-1}, corroborated such hydrophilic behavior. Additionally, the CO_2 capture was equal to 9.3 wt% for activated $Fe(pz)[Pt(CN)_4]$, a higher value in comparison to other lead MOFs like the NOTT-400 (4.4 wt%), despite this latter one exhibits a larger BET surface area (1356 m^2 g^{-1}) than $Fe(pz)[Pt(CN)_4]$ (BET = 431 m^2 g^{-1}). When the CO_2 capture capability was measured on the partially water-saturated $Fe(pz)[Pt(CN)_4]$ sample, we observed a weight gain from 11.7 wt% (only water uptake) to 14.1 wt% (water + CO_2). This weight increment (2.4 wt%) was attributed to the oversolubility of CO_2. The CO capture on $Fe(pz)[Pt(CN)_4]$ showed a total uptake of 4.7 mmol/g after only 20 min; a result comparable to those for MOFs with much higher BET surface areas, like MOF-74(Mg) (BET = 1957 m^2 g^{-1}; 4.4 mmol g^{-1}). Finally, *in situ* DRIFT experiments exhibited the coordination of CO with open Pt(II) metal sites.

Metal-organic frameworks (MOFs)[1] or porous coordination polymers (PCPs)[2] are hybrid and crystalline materials synthesized from discrete metal cations (or metal clusters) and organic polydentate ligand donors (typically carboxylates),[3] resulting in 1D, 2D or 3D arrangements.[4] Some MOFs have shown many interesting properties; for instance, ultra-high porosity, large surface area, uncommon flexibility, and resistance to some harsh conditions like strong acidic or basic media, moisture, heat, and light, among others.[5] In addition, MOFs have a designable or, tuneable micro-porosity, depending essentially on the structure of their organic ligands (main building units).[6] Indeed, in order to gain even more control over their structure and properties, MOFs can be modified *'a la carte' via* post-synthetic transformations, as it was masterfully described by Humphrey and co-workers.[7] Besides, MOFs have been used successfully in various fields of science and technology; for example, as chemical sensors,[8] proton-conducting materials,[9] magnetic materials,[10] heterogeneous catalysts for organic synthesis,[11] as well as molecular-warehouses for gases of interest in chemical industry,[12] like oxygen,[13] hydrogen,[14] and methane.[15] However, the use of novel MOFs to capture gases involved in air pollution and global warming is one of their most important applications and an issue still worthy to be investigated. In the same way, it is a growing field of opportunity for organic, inorganic, environmental, and materials science researchers.[16] In our group, we have investigated relevant host-guest interactions between CO_2 and a selected group of MOF materials (such as HKUST-1, NOTT-400, InOF-1, CAU-10, Mg-CUK-1 and MIL-53(Al)) either, in native form or with pre-adsorbed water, alcohols and/or other polar molecules to increase their CO_2 uptake capability.[17]

In this work, we explore the H_2O, CO_2 and CO adsorption properties of the microporous material $Fe(pz)[Pt(CN)_4]$ (Figure 1).[18] This material is constructed with cyanide (CN) bridges and pyrazine (pz) linkers to form a hybrid bimetallic [Fe-Pt] 3D Hofmann-like coordination polymer, showing a spin transition with a large hysteresis loop, close to room temperature for powder and ultrathin film samples.[19] Accordingly, this material has been used successfully to understand the cooperative spin-crossover phenomena[6,20] in coordination polymers,[21] even upon adsorption of solvents.[22]

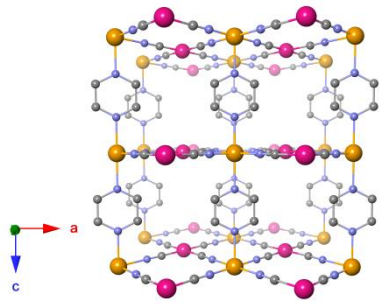

Figure 1. View of the 3D porous coordination polymer Fe(pz)[Pt(CN)$_4$]. The {Fe[Pt(CN)$_4$]}$_\infty$ sheets (002 plane) are connected by pyrazine organic linkers. Colorkey: Fe(yellow), Pt(pink), N(blue), C(grey).

The high-spin state (HS) of Fe(pz)[Pt(CN)$_4$] material was synthesized following a previously published procedure[19a] with few modifications. A 2 mL volume of a H_2O/MeOH (1:1) solution of $Fe(BF_4)_2$ (0.05M) and pyrazine (0.05 M) was added at once to 2 mL of a 0.05 M aqueous solution of $K_2Pt(CN)_4$ at room temperature under agitation. The yellow precipitate obtained was filtered, washed with acetone and dried for 2 hours at 180 °C before powder X-ray diffraction (PXRD) and nitrogen isotherms characterization.

The as-synthesized material Fe(pz)[Pt(CN)$_4$] was initially characterized by PXRD in a Rigaku ULTIMA IV diffractometer with Cu-Kα_1 radiation (λ = 1.54 Å), (Figure 2). It is shown in Figure 2, the as-synthesized PXRD pattern matches with the one previously reported by Kitagawa and co-workers,[6] for high spin state. It is worth mentioning that, with the exception of the N_2 adsorption experiments at 77 K, thermal-induced spin transitions (due to sorption experiments) are not expected.[6,22a]

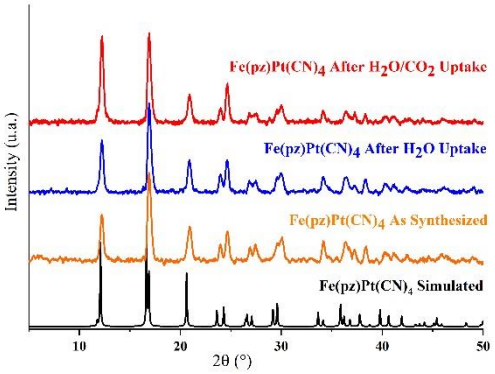

Figure 2. PXRD room temperature comparison of high spin state Fe(pz)[Pt(CN)$_4$] simulated[6] (black line), as synthesized (orange line), after H_2O uptake (blue line) and after H_2O/CO_2 uptake (red line).

Nitrogen (N_2) adsorption isotherms were performed using a Micromeritics ASAP 2020 instrument. These were obtained (at 77 K) in order to calculate the BET surface area ($0.01 < P/P_0 < 0.04$) of approximately 431 m^2/g for the activated material (180 ºC for 2 h under vacuum of 1x10^{-3} bar).

Although Fe(pz)[Pt(CN)$_4$] is synthetized in a mixture of water and MeOH, and a remarkable contribution by Paesani *et al.*,[22a] who computationally demonstrated the average positions of the water molecules inside the MOF pores, the water adsorption properties, structural stability and water cyclability of Fe(pz)[Pt(CN)$_4$] have not been investigated, to the best of our knowledge, until now.

Figure 3 shows the water adsorption isotherm at 25 °C for an activated sample (180 ºC for 2 h under a flow of dry N_2) of Fe(pz)[Pt(CN)$_4$]. The water uptake increased very slowly as a function of increasing the partial pressure of H_2O up to P/P_0 = 0.4 (40 % P/P_0). After this point, the graph displayed a marked change in the slope, which probably indicates two different adsorption domains. The total water uptake was equal to 14.6 wt% (8.12 mmol/g) at 0.9 P/P_0 (90 % P/P_0).

The kinetic diameter of water (~2.7 Å) is smaller than the square-like channels of Fe(pz)[Pt(CN)$_4$] (3.9 Å x 4.2 Å). Thus, the hysteresis loop observed could be explained in terms of the adsorbent-adsorbate interactions. In order to understand this interaction, the isosteric enthalpy of adsorption of water was calculated by applying the Clausius-Clapeyron relation on the adsorption equilibrium data measured at two different temperatures. Thus, an additional water adsorption isotherm was performed at 35 °C (see Fig. S1). The ΔH_{ads} obtained was -55 kJ mol^{-1}. This value is higher than the water enthalpy of vaporization (-41 kJ mol^{-1} at 25 °C), which corroborates the high affinity of water molecules for Fe(pz)[Pt(CN)$_4$]. A PXRD experiment on Fe(pz)[Pt(CN)$_4$] after the water adsorption experiment (see Figure 2) exhibited the retention of the crystallinity and therefore, the structural stability of Fe(pz)[Pt(CN)$_4$] towards water.

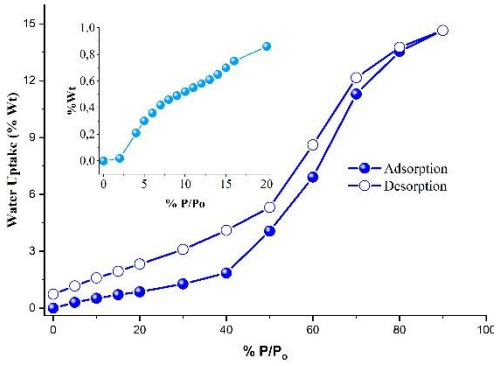

Figure 3. Water adsorption-desorption isotherm for Fe(pz)[Pt(CN)$_4$] performed at 25 °C.

To test the water adsorption-desorption recyclability of Fe(pz)[Pt(CN)$_4$] water sorption isotherms were measured, on the same sample, for 4 cycles at 25 °C (see Figure 4). These results showed no apparent reduction in capacity over four cycles and shown the complete regeneration of the material solely by evacuating without any thermal activation. In order to investigate any sample degradation, we have carried out PXRD experiments on the Fe(pz)[Pt(CN)$_4$] sample after these cycling experiments. Fig. S7 (see SI) confirms that the crystallinity of the sample after each water adsorption–desorption experiment (4 cycles) was retained, and the BET surface area of this sample was also maintained (425 m^2/g).

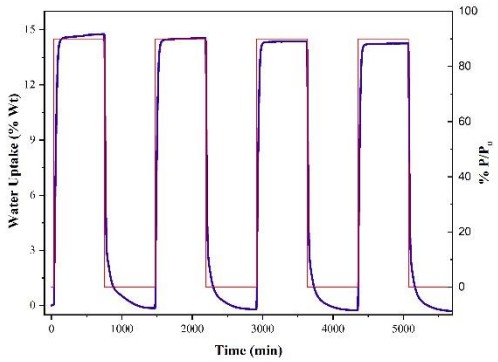

Figure 4. H_2O uptake cycles (adsorption-desorption) at 25 °C for Fe(pz)[Pt(CN)$_4$].

In a closer inspection of the water adsorption isotherm, from 0 to approximately 20 % P/P_0 (see inset on Figure 3), the material exhibits an apparent hydrophobic behaviour (since the water uptake is not very high). In order to corroborate such behaviour, we decided to perform the adsorption of a non-polar molecule (cyclohexane) in Fe(pz)[Pt(CN)$_4$]. Then, Figure 5 shows the cyclohexane adsorption isotherm at 25 °C for an activated sample (180 ºC for 2 h under a flow of dry N_2) of Fe(pz)[Pt(CN)$_4$]. The cyclohexane uptake increased relatively fast as a function of increasing partial pressure of cyclohexane from 0 to approximately 5 P/P_0 (cyclohexane uptake of 0.59 wt%, see Figure 5). Later, form that point until the end of the experiment (85 % P/P_0) there is a constant uptake increase to reach a total cyclohexane uptake of 2.39 wt% (0.28 mmol/g). When comparing the total water uptake (8.12 mmol/g) with the total cyclohexane uptake (0.28 mmol/g), it is evident that Fe(pz)[Pt(CN)$_4$] is a hydrophilic MOF material. In addition, the desorption phase for cyclohexane showed no hysteresis indicating a poor interaction of this molecule with the channels of the material. Finally, we carried out another cyclohexane adsorption isotherm to estimate the isosteric enthalpy of adsorption for

cyclohexane (as previously described, *vide supra*). The ΔH_{ads} obtained was -33 kJ mol^{-1}, which demonstrates a weaker interaction in comparison to water (-55 kJ mol^{-1}).

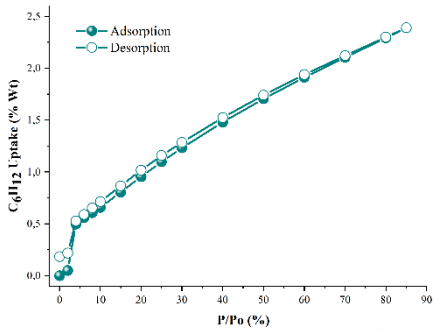

Figure 5. Cyclohexane adsorption-desorption isotherm for Fe(pz)[Pt(CN)$_4$] performed at 25 °C.

Kinetic and isothermal CO_2 experiments (with a CO_2 flow of 60 mL/min) were performed on an activated sample (180 ºC for 2 h under a flow of dry N_2) of Fe(pz)[Pt(CN)$_4$] (Figure 6) at 25 °C and anhydrous conditions. Under these conditions the maximum amount of CO_2 captured was equal to 9.3 wt% (rapidly reached after only 5 min) and it was constant until the end of the experiment (25 min). Surprisingly, this CO_2 uptake is considerably higher (under kinetic conditions) than, for example, the CO_2 uptake for NOTT-400 (4.4 wt%).[17b] NOTT-400 is a MOF material that exhibits a much larger BET surface area (1356 m^2/g) than Fe(pz)[Pt(CN)$_4$] (BET = 431 m^2/g). In order to have a comparative CO_2 capture to other benchmark MOFs, we constructed a CO_2 capture graph (under similar conditions), taking into consideration the BET surface area. This graph is presented in the SI (see Figure S8).

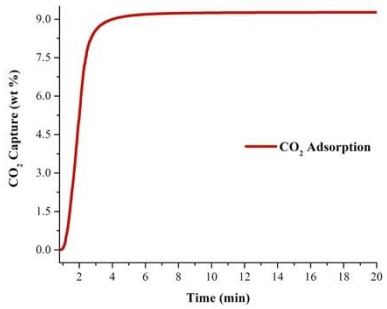

Figure 6. CO_2 kinetic uptake experiment for Fe(pz)[Pt(CN)$_4$] at 25 °C with a CO_2 flow of 60 mL/min.

In additional, we performed CO_2 adsorption-desorption cycles at 25 °C (Figure 7) on an activated sample of Fe(pz)[Pt(CN)$_4$]. These cycles demonstrated that Fe(pz)[Pt(CN)$_4$] did not lose its CO_2 capture capacity after 3 cycles and the BET surface area of this sample was also retained (433 m^2/g).

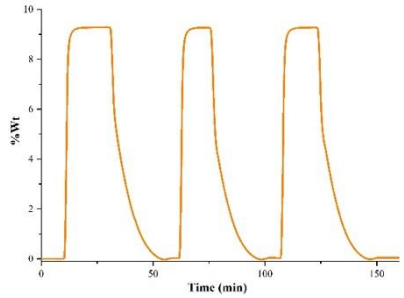

Figure 7. CO_2 uptake cycles (adsorption-desorption) at 25 °C for Fe(pz)[Pt(CN)$_4$].

Our group has been investigating the confinement of small amounts of polar molecules (*e.g.*, H_2O, EtOH, MeOH, DMF, etc.) to enhance the CO_2 adsorption properties of hydroxo (μ_2-OH) functionalized MOF materials.[16,17] Indeed, the key to achieve such CO_2 capture enhancement is the formation of hydrogen bonds between these polar molecules and the hydroxo functional group. Thus, in the case of Fe(pz)[Pt(CN)$_4$] we decided to investigate the oversolubility of CO_2 within the pores of Fe(pz)[Pt(CN)$_4$] partially-saturated with water. The oversolubility of confined solvents considerably modifies their viscosity, density, dielectric constant, and specific heat.[23] As a remarkable example, Garcia-Garibay[24] showed in a MOF entitled UCLA-R3 that the confinement of DMF significantly enhanced the viscosity of this solvent up to 4 orders of magnitude.

Therefore, an activated sample (180 ºC for 2 h under a flow of dry N_2) of Fe(pz)[Pt(CN)$_4$] was partially-saturated (70 % P/P_0) with water (by a kinetic and isothermal experiment; N_2 as the carrier gas of water vapour), see Figure 8. Although at 70 % P/P_0 does not correspond to the fully water saturated point, it is a very close point to water saturation (see Figure 3). From 0 min to approximately 50 min the water uptake reached a value of 11.3 wt% (see Figure 8). From 50 min to 70 min the water uptake reached stability with a total uptake of 11.7 wt%, in good agreement with the water adsorption isotherm (see Figure 3). At 80 min of running the kinetic water adsorption experiment, the N_2 flow was switched to CO_2 and sharp weight gain was clearly observed from 11.7 to 14.1 wt%, see Figure 8. This final uptake (H_2O+CO_2) remained constant until the end of the experiment (100 min). A PXRD experiment (see Figure 2) showed the retention of the crystal structure of this MOF material after the experiment.

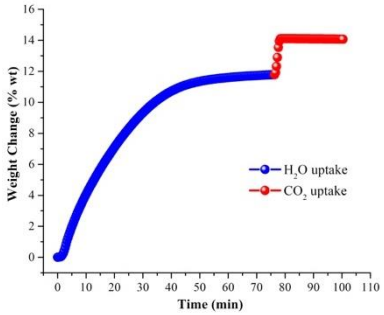

Figure 8. Kinetic uptake experiments carried out at 70 % P/P_0 at 25 °C; H_2O (blue line) and H_2O+CO_2 (red line).

We postulate that this extra weight increase of 2.4 wt% represents the oversolubility of CO_2 in the partially water-saturated (70 % P/P_0) Fe(pz)[Pt(CN)$_4$] sample. In order to corroborate this hypothesis, a similar kinetic experiment was performed Fig. S10 (see SI), where the water uptake was recorded without changing the N_2 flow to CO_2. Further computational calculations will be carried out in order to win more insights on this phenomenon.

Finally, we investigated the CO capture properties of Fe(pz)[Pt(CN)$_4$] by performing a kinetic and isothermal CO experiment (with a CO flow 60 mL/min; CO (5%) in He) on an activated (180 ºC for 2 h under a flow of dry N_2) sample of Fe(pz)[Pt(CN)$_4$]. Figure 9 shows the CO adsorption (at 25 ºC) in which from the beginning of the experiment to 5 min, the CO uptake rapidly reached a value of approximately 10.2 wt%. From 5 min to 11 min the CO uptake augmented to 12.5 wt%, to finally reach a total CO capture of 13.2 wt% (4.7 mmol/g, at 20 min; see Figure 9). This CO uptake is comparable to MOF materials with a much higher BET surface area such as MOF-74(Mg) (BET = 1957 m^2/g; CO uptake of 4.4 mmol/g).[25]

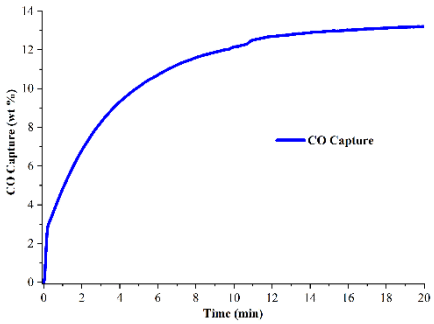

Figure 9. CO kinetic uptake experiment for Fe(pz)[Pt(CN)$_4$] at 25 °C with a CO flow 60 mL/min; CO (5%) in He.

In order to investigate the potential impact of Pt(II) sites and their role in sorption dynamics, *in situ* Diffuse Reflectance Infrared Fourier Transform (DRIFT) experiments upon the adsorption of CO within Fe(pz)[Pt(CN)$_4$] were performed. Thus, CO adsorption was followed by FTIR spectroscopy in a Thermo Scientific Nicolet iS50 (DTGS detector working at 4 cm^{-1}resolution and 128 scans) in an environmentally controlled PIKE DifussIR DRIFT cell with a KBr window at ambient pressure. The sample was activated *in situ* at 180 °C for 2 h under a He flow (30 mL/min). 5% CO/He flow (30 mL min^{-1}) at 25 °C was used and the spectra of the solid were collected at different times. In all cases, reported spectra consider the spectrum of the activated Fe(pz)[Pt(CN)$_4$] prior to CO adsorption. The spectra shown in Figure 10 present the spectral region where carbonyls adsorbed on metal phases can be found. The Fe(pz)[Pt(CN)$_4$] spectrum shows different peaks between 2250 and 2100 cm^{-1} which are associated to the stretching vibrational modes of the C≡N bound in the cyanide (CN) bridges and pyrazine (pz) linkers. After the CO adsorption, the solid features five principal peaks, 2193, 2158, 2116, 2090 and 1837 cm^{-1}. The broad peaks centred at 2158 and 2116 cm^{-1} are associated to the CO gas phase, while the peak at 2090 cm^{-1} is assigned to the linearly-coordinated CO on Pt(II), and 1837 cm^{-1} peak related to bridging CO on Pt(II).[26] Finally, the peak observed at 2193 cm^{-1} is associated to CO coordinated to Pt^{n+} sites (in this case Pt^{2+}), which are generally expected at frequencies above than 2100 cm^{-1}.[26-27]

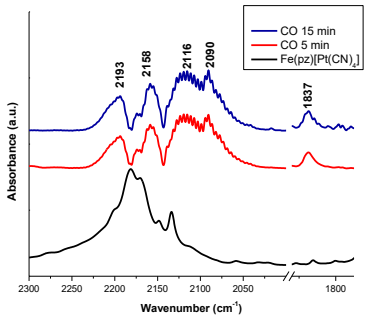

Figure 10. DRIFTs spectra collected at different CO adsorption times over activated Fe(pz)[Pt(CN)$_4$] at 25 °C, in the region between 2300 and 1900 cm^{-1}.

As concluding remarks, it is worth highlighting the below enlisted findings: (*i*) the hybrid 3D microporous coordination polymer Fe(pz)[Pt(CN)$_4$] exhibited an outstanding structural stability and recyclability after all adsorption-desorption cycles of water and water + CO_2 (demonstrated by PXRD); (*ii*) Fe(pz)[Pt(CN)$_4$] showed to have a hydrophilic nature, which was corroborated by comparative experiments of water (polar) and cyclohexane (non-polar) adsorption experiments; (*iii*) the Fe(pz)[Pt(CN)$_4$] adsorbed more CO_2 and CO in comparison to other MOFs with much high larger BET surface areas, such as the NOTT-400 and MOF-74(Mg), respectively and by *in situ* DRIFT experiments we demonstrated the interaction (coordination) of CO with open Pt(II) metal sites; and (*iv*) we postulate the oversolubility of CO_2 within the partially water-saturated Fe(pz)[Pt(CN)$_4$] sample. Future computational calculations studies will provide more insights on these relevant and exciting adsorption properties of Fe(pz)[Pt(CN)$_4$].

ASSOCIATED CONTENT

Supporting Information

The Supporting Information is available free of charge on the ACS Publications website.

Isotherms, CO uptake charts, sorption-desorption profiles, PXRDs, (PDF).

AUTHOR INFORMATION

Corresponding Authors

*E-mail: aij@xanum.uam.mx, mathieu.gonidec@icmcb.cnrs.fr, argel@unam.mx

ORCID

Alejandro Islas-Jácome: 0000-0003-0975-5904
Mathieu Gonidec: 0000-0002-0187-1305
Ilich A. Ibarra: 0000-0002-3995-9126

Notes

The authors declare no competing financial interest

ACKNOWLEDGMENT

The authors thank Dr. A. Tejeda-Cruz (powder X-ray; IIM-UNAM), A. Gómez-Cortés (DRIFT, IF-UNAM). CONACyT (1789), PAPIIT UNAM (IN101517), México for financial support. A.I.-J. acknowledges PRODEP-SEP (511-6/18-8354) and CONACyT-SEP CB-2017-2018 (A1-S-32582) for financial support. M. G. acknowledges (ARN-10-IDEX-03-02). E. G.-Z. thanks CONACyT (236879) for financial support. D. A.-A. thanks CONACyT for providing scholarship (C.V. 733615). J. H. G.-E. thanks CONACyT (073096).

REFERENCES

(1) Zhou, H.-C.; Long, J. R.; Yaghi, O. M. Introduction to Metal−Organic Frameworks. *Chem. Rev.* **2012**, *112*, 673–674.
(2) Das, S.; Heasman, P.; Ben, T.; Qiu, S. Porous Organic Materials: Strategic Design and Structure−Function Correlation. *Chem. Rev.* **2017**, *117*, 1515–1563.
(3) Lin, X.; Telepeni, I.; Blake, A. J.; Dailly, A.; Brown, C. M.; Simmons, J. M.; Zoppi, M.; Walker, G. S.; Thomas, K. M.; Mays, T. J.; Hubberstey, P.; Champness, N. R.; Schröder, M. High Capacity Hydrogen Adsorption in Cu(II) Tetracarboxylate Framework Materials: The Role of Pore Size, Ligand Functionalization, and Exposed Metal Sites. *J. Am. Chem. Soc.* **2009**, *131*, 2159–2171.
(4) Janiak, C. Engineering coordination polymers towards applications. *Dalton Trans.* **2003**, *14*, 2781–2804.
(5) James, S. L. Metal-organic frameworks. *Chem. Soc. Rev.* **2003**, 32, 276–288.
(6) Ohba, M.; Yoneda, K.; Agustí, G.; Muñoz, M. C.; Gaspar, A. B.; Real, J. A.; Yamasaki, M.; Ando, H.; Nakao, Y.; Sakaki, S.; Kitagawa, S. Bidirectional Chemo-Switching of Spin State in a Microporous Framework. *Angew. Chem. Int. Ed.* **2009**, *48*, 4767–4771.
(7) Dunning, S. G.; Reynolds III, J. E.; Walsh, K. M.; Kristek, D. J.; Lynch, V. M.; Kunal, P.; Humphrey, S. M. Direct, One-Pot Syntheses of MOFs Decorated with Low-Valent Metal-Phosphine Complexes. *Organometallics* **2019**, *38*, 3406–3411.
(8) Meng, Q.; Xin, X.; Zhang, L.; Dai, F.; Wang, R.; Sun, D. A multifunctional Eu MOF as a fluorescent pH sensor and exhibiting highly solvent-dependent adsorption and degradation of rhodamine B. *J. Mater. Chem. A* **2015**, *3*, 24016–24021.
(9) Ramaswamy, P.; Wong, N. E.; Shimizu, G. K. H. MOFs as proton conductors – challenges and opportunities. *Chem. Soc. Rev.* **2014**, *43*, 5913–5932.
(10) Zeng, M.-H.; Yin, Z.; Tan, Y.-X.; Zhang, W.-X.; He, Y.-P.; Kurmoo, M. Nanoporous Cobalt (II) MOF Exhibiting Four Magnetic Ground States and Changes in Gas Sorption upon Post-Synthetic Modification. *J. Am. Chem. Soc.* **2014**, *136*, 4680–4688.
(11) Zhu, L.; Liu, X.-Q.; Jiang, H.-L.; Sun, L.-B. Metal-Organic Frameworks for Heterogeneous Basic Catalysis. *Chem. Rev.* **2017**, *117*, 8129–8176.
(12) Sánchez-Serratos, M.; Álvarez, J. R.; González-Zamora, E.; Ibarra, I. A. Porous Coordination Polymers (PCPs): New Platforms for Gas Storage. *J. Mex. Chem. Soc.* **2016**, *60*, 43–57.
(13) Kitaura, R.; Kitagawa, S.; Kubota, Y.; Kobayashi, T. C.; Kindo, K.; Mita, Y.; Matsuo, A.; Kobayashi, M.; Chang, H.-C.; Ozawa, T. C.; Suzuki, M.; Sakata, M.; Takata, M. Formation of a One-Dimensional Array of Oxygen in a Microporous Metal-Organic Solid. *Science* **2005**, *298*, 2358–2361.
(14) Yan, Y.; Telepeni, I.; Yang, S., Lin, X.; Kockelmann, W.; Dailly, A.; Blake, A. J.; Lewis, W.; Walker, G. S.; Allan, D.R.; Barnett, S. A.; Champness, N. R.; Schröder, M. Metal-Organic Polyhedral Frameworks: High H_2 Adsorption Capacities and Neutron Powder Diffraction Studies. *J. Am. Chem. Soc.* **2010**, *132*, 4092–4094.

(15) Li, B.; Wen, H.-M.; Zhou, W.; Xu, J. Q.; Chen, B. Porous Metal-Organic Frameworks: Promising Materials for Methane Storage. *Chem.* **2016**, *1*, 557.
(16) González-Zamora, E.; Ibarra, I. A. CO_2 capture under humid conditions in metal–organic frameworks. *Mater. Chem. Front.* **2017**, *1*, 1471.
(17) (a) Peralta, R. A.; Alcántar-Vásquez, B.; Sánchez-Serratos, M.; González-Zamora, E.; Ibarra, I. A. Carbon dioxide capture in the presence of wáter vapour in InOF-1. *Inorg. Chem. Front.* **2015**, *2*, 898–903. (b) Álvarez, J. R.; Peralta, R. A.; Balmaseda, J.; González-Zamora, E.; Ibarra, I. A. *Inorg. Chem. Front.* **2015**, *2*, 1080–1084. (c) Sánchez-Serratos, M.; Bayliss, P. A.; Peralta, R. A.; González-Zamora, E.; Lima, E.; Ibarra. I. A. CO_2 capture in the presence of water vapour in MIL-53(Al). *New J. Chem.* **2016**, *40*, 68–72. (d) Zárate, A.; Peralta, R. A.; Bayliss, P. A.; Howie, R.; Sánchez-Serratos, M.; Carmona-Monroy, P.; Solis-Ibarra, D.; González-Zamora, E.; Ibarra, I. A. CO_2 capture under humid conditions in NH_2-MIL-53(Al): the influence of the amine functional group *RSC Advances* **2016**, *6*, 9978–9983. (e) Sánchez-González, E.; Raziel Álvarez, J.; Peralta, R. A.; Campos-Reales-Pineda, A.; Tejeda-Cruz, A.; Lima, E.; Balmaseda, J.; González-Zamora, E.; Ibarra, I. A. Water Adsorption Properties of NOTT-401 and CO_2 Capture under Humid Conditions. *ACS Omega* **2016**, *1*, 305–310. (f) Peralta, R. A.; Campos-Reales-Pineda, A.; Pfeiffer, H.; Álvarez, J. R.; Antonio Zárate, J.; Balmaseda, J.; González-Zamora, E.; Martínez, A.; Martínez-Otero, D.; Jancik, V. Ibarra, I. A. *Chem. Commun.* **2016**, *52*, 10273–10276. (g) Raziel-Alvarez, J.; Sánchez-González, E.; Pérez, E.; Schneider-Revueltas, E.; Martínez, A.; Tejeda-Cruz, A.; Islas-Jácome, A.; González-Zamora, E.; Ibarra, I. A. Structure stability of HKUST-1 towards water and ethanol and their effect on its CO_2 capture properties. *Dalton Trans*. **2017**, *46*, 9192–9200. (h) Sánchez-González, E.; González-Zamora, E.; Martínez-Otero, D.; Jancik, V.; Ibarra. I. A. *Inorg. Chem.* **2017**, *56*, 5863–5872. (i) González-Martínez, G. A.; Antonio Zárate, J.; Martínez, A.; Sánchez-González, E.; Raziel Álvarez, J.; Lima, E.; González-Zamora, E.; Ibarra, I. A. Confinement of alcohols to enhance CO_2 capture in MIL-53(Al). *RSC Adv.* **2017**, *7*, 24833–24840. (j) Sánchez-González, E.; Mileo, P. G. M.; Raziel Álvarez, J.; González-Zamora, E.; Maurin, G.; Ibarra, I. A. Confined methanol within InOF-1: CO_2 capture enhancement *Dalton Trans*. **2017**, *46*, 15208–15215. (k) Álvarez, J. R.; Mileo, P. G. M.; Sánchez-González, E.; Zárate, J. A.; Rodríguez-Hernández, J.; González-Zamora, E.; Maurin, G.; Ibarra, I. A. Adsorption of 1-Propanol in the Channel-Like InOF-1 Metal–Organic Framework and its Influence on the CO_2 Capture Performances. *J. Phys. Chem. C* **2018**, *122*, 5566–5577. (l) González-Martínez, G. A.; Jurado-Vázquez, T.; Solís-Ibarra, D.; Vargas, B.; Sánchez-González, E.; Martínez, A.; Vargas, R.; González-Zamora, E.; Ibarra, I. A. Confinement of H_2O and EtOH to enhance CO_2 capture in MIL-53(Al)-TDC. *Dalton Trans*. **2018**, *47*, 9459–9465. (m) Sagastuy-Breña, M.; Mileo, P. G. M.; Sánchez-González, E.; Reynolds III, J. E.; Jurado-Vázquez, T.; Balmaseda, J.; González-Zamora, E.; Devautour-Vinot, S.; Humphrey, S. M.; Maurin, G.; Ibarra, I. A. Humidity-induced CO_2 capture enhancement in Mg-CUK-1. *Dalton Trans.* **2018**, *47*, 15827–15834. (n) López-Cervantes, V. B.; Sánchez-González, E.; Jurado-Vázquez, T.; Tejeda-Cruz, A.; González-Zamora, E.; Ibarra, I. A. CO_2 adsorption under humid conditions: Self-regulated water content in CAU-10. *Polyhedron* **2018**, *155*, 163–169. (o) Sanchez-González, E.; Mileo, P. G. M.; Sagastuy-Breña, M.; Raziel-Alvarez, J.; Reynolds III, J. E.; Villarreal, A.; Gutierrez-Alejandre, A.; Ramírez, J.; Balmaseda, J.; Gonzalez-Zamora, E.; Maurin, G.; Humphrey, S. M.; Ibarra, I. A. Highly reversible sorption of H_2S and CO_2 by an environmentally friendly Mg-based MOF. *j. Mater. Chem. A* **2018**, *6*, 16900–16909. (p) Zárate, A.; Sánchez-González, E.; Jurado-Vázquez, T.; Gutiérrez-Alejandre, A.; González-Zamora, E.; Castillo, I.; Maurin, G.; Ibarra, I. A. *Chem. Commun.* **2019**, *55*, 3049–3052. (q) Sánchez-Bautista, J. E.; Landeros-Rivera, B.; Jurado-Vázquez, T.; Martínez, A.; González-Zamora, E.; Balmaseda, J.; Vargas, R.; Ibarra, I. A. CO_2 capture enhancement for InOF-1: confinement of 2-propanol. *Dalton Trans.* **2019**, *48*, 5176–5182. (r) Lara-García, H. A.; Landeros-Rivera, B.; González-Zamora, E.; Aguilar-Pliego, J.; Gómez-Cortés, A.; Martínez, A.; Vargas, R.; Diaz, G.; Ibarra, I. A. Relevance of hydrogen bonding in CO_2 capture enhancement within InOF-1: an energy and vibrational análisis. *Dalton Trans.* **2019**, *48*, 8611–8616. (s) Díaz-Ramírez, M. L.; Sánchez-González, E.; Raziel-Alvarez, J.; González-Martínez, G. A.; Horike, S.; Kadota, K.; Sumida, K.; Gonzalez-Zamora, E.; Springuel-Huet, M.-A.; Gutiérrez-Alejandre, A.; Jancik, V.; Furukawa, S.; Kitagawa, S.; Ibarra, I. A.; Lima, E. Partially fluorinated MIL-101(Cr): from a miniscule structure modification to a huge chemical environment transformation inspected by ^{129}Xe NMR. *J. Mater. Chem. A.* **2019**, *7*, 15101–15112. (t) Zarate, J. A.; Sánchez-González, E.; Williams, D. R.; González-Zamora, E.; Martis, V.; Martínez, A.; Balmaseda, J.; Maurin, G.; Ibarra, I. A. High and energy-efficient reversible SO_2 uptake by a robust Sc(III)-based MOF. *J. Mater. Chem. A* **2019**, *7*, 15580–15584.
(18) Levchenko, G.; Gaspar, A. B.; Bukin, G.; Berezhnaya, L.; Real, J. A. Pressure Effect Studies on the Spin Transition of Microporous 3D Polymer [Fe(pz)Pt(CN)$_4$]. *Inoorg. Chem.* **2018**, *57*, 8458–8464.
(19) (a) Agustí, G.; Cobo, S.; Gaspar, A.B.; Molnár, G.; Moussa, N.O.; Szilágyi, P.A.; Pálfi, v.; Vieu, C.; Muñoz, M.C.; Real, J.A.; Bousseksou, A. Thermal and Light-Induced Spin Crossover Phenomena in New 3D Hofmann-Like Microporous Framewroks Produced As Bulk Materials and Nanopatterned Thin films. *Chem. Mater.* **2008**, 20, 21, 6721-6732. (b)Bartual-Murgui, C.; Cerf, A.; Thibault, C.; Vieu, C.; Salmon, L.; Molnár, G.; Bousseksou, A. SERS-active substrates for investigating ultrathin spin-crossover films. *Microelectronic Engineering* **2013**, *111*, 365–368.
(20) (a) Delgado, T.; Tissot, A.; Besnard, C.; Guénée, L.; Pattison, P.; Hauser, A. Structural Investigation of the High Spin - Low Spin Relaxation Dynamics of the Porous Coordination Network [Fe(pz)Pt(CN)$_4$]·2.6H$_2$O. *Chem. Eur. J.* **2015**, *21*, 3664–3670. (b) Delgado, T.; Enachescu, C.; Tissot, A.; Guénée, L.; Hauser, A.; Besnard, C. The influence of the sample dispersion on a solid surface in the thermal spin transition of [Fe(pz)Pt(CN)4] nanoparticles. *Phys. Chem. Chem. Phys.* **2018**, *20*, 12493–12502.
(21) Niel, V.; Martinez-Agudo, J. A.; Muñoz, M. C.; Gaspar, A. B.; Real, J. A. Cooperative Spin Crossover Behavior in Cyanide-Bridged Fe(II)-M(II) Bimetallic 3D Hofmann-like Networks (M = Ni, Pd, and Pt). *Inoorg. Chem.* **2001**, *40*, 3838–3839.
(22) (a) Pham, C. H.; Cirera, J.; Paesani, F. Molecular Mechanisms of Spin Crossover in the {Fe(pz)[Pt(CN)$_4$]} Metal−Organic Framework upon Water Adsorption. *J. Am. Chem. Soc.* **2016**, *138*, 6123–6126. (b) Pham, C. H.; Paesani, F. Spin Crossover in the {Fe(pz)[Pt(CN)$_4$]} Metal−Organic Framework upon Pyrazine Adsorption. *J. Phys. Chem. Lett.* **2016**, *7*, 4022–4026. (c) Sawczak, M.; Jendrzejewski, R.; Maskowicz, D.; García, Y.; Ghosh, A. C.; Gazda, M.; Czechowski, J.; Sliwinski, G. Nanocrystalline Polymer Impregnated [Fe(pz)Pt(CN)$_4$] Thin Films Prepared by Matrix-Assisted Pulsed Laser Evaporation. *Eur. J. Inorg. Chem.* **2019**, 3249–3255.
(23) (a) Hernandez-Rojas, J.; Calvo, F.; Bretón, J.; Gomez-Llorente, J.M. Confinement Effects on Water Clusters Inside Carbon Nanotubes. *J. Phys. Chem. C* **2012**, *116*, 17019−17028. (b) Chakraborty, S.; Kumar, H.; Dasgupta, C.; Maiti, P.K. Confined Water: Structure, Dynamics, and Thermodynamics. *Acc. Chem. Res.* **2017**, *50*, 2139−2146.
(24) Jiang, X.; Duan, H. B.; Khan, S. I.; Garcia-Garibay, M. A. Diffusion-Controlled Rotation of Triptycene in a Metal-Organic Framework (MOF) Sheds Light on the Viscosity of MOF-Confined Solvent. *ACS Cent. Sci.* **2016**, *2*, 608−613.
(25) Bloch, E. D.; Hudson, M. R.; Mason, J. A.; Chavan, S.; Crocellá, V.; Howe, J. D.; Lee, K.; Dzubak, A. L.; Queen, W. L.; Zadrozny, J. M.; Geier, S. J.; Lin, L.-C.;Gagliardi, L.; Smit, B.; Neaton, J. B.; Bordiga, S.; Brown, C. M.; Long, J. R. Reversible CO Binding Enables Tunable CO/H_2 and CO/N_2 Separations in Metal–Organic Frameworks with Exposed Divalent Metal Cations. *J. Am. Chem. Soc.* **2014**, *136*, 10752–10766.
(26) Whitford C. L., Stephenson C. J., Gómez-Gualdrón D. A., Hupp J. T., Farha O. K, Snurr R. Q., Stair P. C. Elucidating the Nanoparticle–Metal Organic Framework Interface of Pt@ZIF-8 Catalysts. *J. Phys. Chem. C*, **2017**, *121*, 25079–25091.
(27) Hadjiivanov K. I., IR study of CO and H_2O co-adsorption on Pt^{n+}/TiO_2 and Pt/TiO_2 samples, *J. Chem. Soc., Faraday Trans.*, **1998**, *94*, 1901–1904.